Title

Linking Neural Dynamics of Prediction to Decision: Evidence for N400-Drift-Diffusion Parameters Relationship

Permalink

https://escholarship.org/uc/item/4g81q9hr

Journal

Proceedings of the Annual Meeting of the Cognitive Science Society, 48(0)

Authors

Tumanyants, Anna

Straube, Benjamin

He, Yifei

Publication Date

2026

Linking Neural Dynamics of Prediction to Decision: Evidence for N400-Drift-Diffusion Parameters Relationship

Anna Tumanyants (anna.tumanyants@uni-marburg.de)[1], Benjamin Straube[1], Yifei He[1]
[1]Department of Psychiatry and Psychotherapy, Philipps University Marburg

Abstract

Prediction is central to language comprehension, yet how neural markers of prediction translate into decision behavior remains unclear. We combined EEG with drift-diffusion modeling (DDM) to dissociate prediction-specific mechanisms from semantic priming facilitation effects. Participants (N=30) completed a lexical decision task following either one or three semantically related primes, manipulating prediction strength while holding semantic relatedness constant. The three-prime context elicited early prediction-sensitive activity (eN400, 200–300 ms) alongside classic N400 effects. Critically, DDM revealed a double dissociation: classic N400 predicted drift rate, while eN400 predicted boundary separation, reflecting different computational pathways. These findings demonstrate that even minimal predictive context (three primes) engages early neural processing. Moreover, the observed neurocomputational dissociation between neural indices and decision parameters supports hierarchical predictive accounts of language comprehension by specifying not only whether predictive context matters, but when it influences semantic processing and which task-relevant decision mechanisms it modulates.

Keywords: semantic priming; predictive processing; EEG; N400; drift-diffusion modeling

Introduction

Prediction is a fundamental mechanism that enhances language comprehension by making it faster, more efficient and adaptive. Previous research has examined prediction in language processing from either neural or behavioral perspectives (see Ryskin & Nieuwland, 2023), but both angles are rarely integrated, leaving the relationship between neural markers and behavior unclear. In this study, we aim to dissociate predictive mechanisms in the context of semantic priming and link behavioral modeling methods with neural data to demonstrate their complementary strengths.

From a neural perspective, prediction effects in language comprehension are typically studied using the N400 component (Kutas & Federmeier, 2011), not only in terms of amplitude modulation but also onset latency. For instance, in a seminal study by Lau and colleagues (2013), the authors manipulated predictability with the global proportion of related prime-target combinations. They showed that high vs. low proportion blocks led to enhanced N400 effect for related vs. unrelated targets. Moreover, the N400 effect in the high proportion condition had an earlier onset latency (205–240 ms), which the authors attributed to form-level prediction similar to the N250 in masked priming studies. Similarly, in a word priming study, Luka & Van Petten (2014) found an early N400 facilitation effect of strongly related words presented sequentially in the 200–300 ms window, reflecting facilitated processing when predictions were confirmed. Together, these studies suggest that predictive context can modulate ERP responses earlier than the canonical N400 window. This distinction between early and late N400 effects, as induced by global predictability manipulation, may represent qualitatively different processes within a hierarchical predictive coding framework in which prediction operates at different levels and timescales (Kuperberg & Jaeger, 2016; Bornkessel-Schlesewsky & Schlesewsky, 2019).

In this study, extending Lau, Holcomb and Kuperberg's (2013) work, we designed a novel semantic priming paradigm that manipulates the degree of prediction in a minimal, local context. In classic semantic priming, a semantically related vs. unrelated target commonly leads to facilitated processing: faster reaction times (RTs) and reduced N400 amplitudes. However, these behavioral and event-related potential (ERP) effects could be driven by either predictive or retrieval-based processes. Here, we introduce a condition with three semantically related primes (long condition), in addition to the classic one-prime target combinations (short condition). Crucially, through the successive presentation of related words, the long condition creates a local context that enhances predictive probability of a related target, while the prime-target semantic relatedness remains unaffected. Thus, by comparing neural and behavioral responses of semantic priming (related vs. unrelated targets) between the short and long conditions, we aim to dissociate prediction effects from the effects of semantic relatedness. Regarding the ERPs, we expect similar modulation of the semantic priming N400 effects following Lau and colleagues (2013): enhanced prediction from the long condition will lead to more pronounced N400 priming effect, and potentially an early instance of the N400 effect.

From a behavioral perspective, predictive facilitation in language processing is typically reflected as shortened RTs and/or increased accuracy. However, these raw behavioral measures cannot sufficiently explain the mechanism underlying behavioral decisions. The drift-diffusion model (DDM) offers a robust framework for this purpose (Ratcliff & McKoon, 2008). DDM decomposes RT and accuracy into latent parameters such as drift rate (v), which represents the speed and direction of evidence accumulation toward a decision, and boundary separation (a), which determines the amount of information needed to make a choice. The DDM approach has been extensively applied to classic semantic priming: the priming effect has been commonly reported as

In G. Boleda, I. Dautriche, M. Maldonado, C. Saldana and T. Torrent (Eds.), *Proceedings of the 48th Annual Conference of the Cognitive Science Society*

being primarily driven by increasing drift rate for related vs. unrelated primes and sometimes by other parameters such as reduced boundary separation, depending on task and priming type (Gomez et al., 2013; Kinoshita et al., 2017; Voss et al., 2013).

Notably, despite literature leveraging either the N400 or DDM to investigate the role of contextual facilitation in language processing, it remains unclear how time-resolved ERP components translate into the computations that drive behavioral decisions. Of particular interest are the N400 and its early phase – a prediction-sensitive effect emerging within the broader N400 time-course, previously reported by Lau et al. (2013) and Nieuwland et al. (2020), hereafter referred to as 'eN400'. Here, we address this gap by combining EEG with an ERP-informed DDM (as in Mueller et al., 2017; Nunez et al., 2017) with our paradigm that manipulates local context buildup and contrasts long vs. short prime conditions. Building on our assumption that local predictive context leads to distinct temporal components of the N400, we predict a potential functional dissociation in the ERP-DDM mapping: variability in the classic N400 window may primarily track drift rate, consistent with changes in quality and efficiency of semantic evidence entering the behavioral decision process. By contrast, the eN400 may covary primarily with the rapid adjustments in response caution, reflected through the boundary separation parameter of the DDM.

Methods

Participants

Thirty-two healthy, right-handed, native German speakers aged 18 to 35 years took part in our experiment. One participant who failed vocabulary tests was excluded, leaving a final sample of 31 participants (10 males, $M_{Age} = 26.4$, $SD_{Age} = 4.2$). Our sample size aligns with previous ERP studies with similar designs investigating N400 effects in predictive semantic processing (Lau et al., 2013; Munding et al., 2025). The study was approved by the ethics commission of the University Hospital of Giessen and Marburg.

Due to a technical issue, one participant was excluded from the EEG analysis, leaving a sample of 30 datasets.

Stimuli

Four exemplars of 20 categories of nouns were chosen to match in frequency (SUBTLEX-DE database; Brysbaert et al., 2011) and semantic similarity (vector differences of word embeddings, fast-text model for German (Grave et al., 2018)). Exemplars from each category served as unrelated targets in prime sequences from other categories, for example, the word *dog* (animals category) was used as an unrelated target for *apple* (fruits category).

Design

Based on the classical semantic priming paradigm with one prime and a target (short condition), we introduced a long condition with three primes belonging to the same category (Figure 1). Thus, through the successive exposure to the same-category words in the long condition, participants' expectation of the next word belonging to the same category strengthened. Each of the two experimental lists had 960 trials, equally divided between the long and short conditions. We included both real and pseudowords as targets in our paradigm, although pseudowords were not used in the analysis.

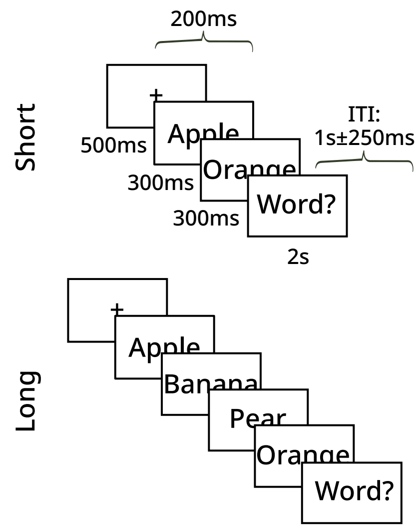

Figure 1: Experimental paradigm. Each trial started with a fixation cross (500 ms), followed by two words in the short condition (top) and four words in the long condition (bottom). Each word was presented for 300 ms with an inter-stimulus interval of 200 ms. At the end of the trial, prompted with a question mark, participants were asked to evaluate whether the previous word was a real word or not, by pressing buttons in a gamepad (corresponding to *yes* (Y) or *no* (N)) (2 s), counterbalanced between participants. The trials were separated by a 1000 ± 500 ms inter-stimulus interval (ITI).

Procedure

Stimuli were presented on a 24.1-inch monitor with PsychoPy (Peirce et al., 2019) on a Windows operating system. A Nintendo controller was used to respond to the stimuli.

One trial consisted of a prime sequence (one or three primes) followed by a target word and a question prompt, as shown in Figure 1. Trials were pseudo-randomized such that no more than three consecutive trials belonged to the same type (e.g., long/short condition and related/unrelated target). Participants indicated whether the last word was a real word or not by pressing the button on the controller.

EEG Data Acquisition

EEG was recorded at 500 Hz using 32 active Ag/AgCl electrodes (actiCAP slim, Brain Products GmbH) following the 10–20 system, amplified with a BrainAmp Standard DC amplifier (Brain Products GmbH). Data were referenced online to FCz with the ground electrode placed on the forehead. Impedance was maintained at or below 25 kΩ. TTL triggers from stimuli and responses, presented via PsychoPy, were recorded concurrently with EEG in BrainVision Recorder (Brain Products GmbH).

EEG Data Preprocessing

The EEG data were preprocessed using EEGLAB (Delorme & Makeig, 2004) and FieldTrip (Oostenveld et al., 2011) in MATLAB (R2023b, Mathworks). Data were downsampled to 250 Hz, re-referenced to the mastoid electrodes (TP9, TP10), and denoised with Zapline-plus (Klug & Kloosterman, 2022). To optimize ICA decomposition, we applied 1 Hz high-pass filtering and used Artifact Subspace Reconstruction (correlation threshold: 0.85, burst rejection: 10 SD). ICA was performed using the extended Infomax algorithm (Pion-Tonachini et al., 2019), and artifactual components were removed with ICLabel. ICA weights were transferred to unfiltered data, band-pass filtered (0.5–100 Hz) and epochs extracted (-200 to 1000 ms). Bad channels (exceeding 20% of trials with amplitude >200 μV) were interpolated, and trials with artifacts were excluded using FieldTrip's automated detection. Mean trial rejection rate across conditions was 12.2% with no significant difference between them. Data were filtered (0.1–40 Hz), and time-locked to the onset of the question prompt (baseline corrected -200 to 0 ms) for ERP analyses.

Data Analysis

We combined conventional statistical methods (Pearson/Spearman correlations, ANOVA), with computational modeling (DDM; Wiecki et al., 2013) for a comprehensive analysis across behavioral and neural levels.

Behavioral Data To exclude meaningless responses, we applied a 100 ms RT lower cutoff. All participants met the minimum accuracy threshold of 80%, ensuring they followed instructions.

RT and accuracy data were analyzed using repeated-measures ANOVAs with Condition (long vs. short) and Target Type (related vs. unrelated) as within-subject factors. RTs were computed from the question prompt onset and averaged within each Condition × Target Type combination for every participant. Accuracy was calculated as the proportion of correct responses in each combination. Effect sizes were quantified using generalized eta squared (η^2G). All analyses were conducted in Python using the *pingouin* package (Vallat, 2018) and used an alpha level of .05.

N400 Mean ERP amplitudes were extracted from the central electrodes (Cz, C3, C4). The N400 component was determined as the mean amplitude within 300–500 ms, calculated from baseline-corrected segments averaged across trials per condition. We performed a 2 × 2 repeated-measures ANOVA on the ERP amplitude values for real word targets with the Condition and Target Type. To decompose the Condition × Target Type interaction, we performed paired-samples t-tests with Bonferroni correction.

eN400 While our main hypotheses centered on the N400, we also analyzed the eN400 component (100 to 300 ms), motivated by previous findings from Lau and colleagues (2013). Mean amplitude was extracted from the same electrodes as for the N400. We calculated Pearson correlations between eN400 and N400 amplitudes using *SciPy* package (Virtanen et al., 2020) in Python. Identical ANOVA models and t-tests used for the N400 analysis were applied.

DDM To fit the DDM, we implemented a hierarchical Bayesian approach using HSSM 0.2.2 package (Fengler et al., in prep.) that uses Markov Chain Monte Carlo (MCMC) sampling. We chose hierarchical models as they are generally more robust with limited observations per participant (Ratcliff & Childers, 2015). We carried out an ERP-informed analysis: across conditions, we extracted single-trial ERP (both eN400 and N400) amplitudes (see above) and entered them into the DDM model as single-trial regressors. Resulting posterior distributions reveal how increasing ERP amplitudes modulate the DDM parameters of interest. Here, based on previous literature (Tumanyants et al., 2025), we focused on the model where only drift rate (v) and boundary separation (a) vary. Parameter estimation used MCMC sampling with 5,000 samples, discarding the first 2,500 samples as burn-in. Model convergence was confirmed using the Gelman-Rubin statistic (r-hat values below 1.01). Statistical inference used posterior parameter distributions compared to zero following standard Bayesian practice. We report posterior means and 95% highest density intervals (significance at <0.05 overlap) to characterize group-level decision processes.

Results

Behavioral Data

15% of all trials were removed where RTs were shorter than 100 ms. One participant was excluded from the behavioral data analysis due to slow responses, leaving a sample of 30 datasets.

Repeated-measures ANOVA on the RT showed no significant main effect of Target Type ($F(1, 29) = 1.52$, $p = .23$, $\eta^2G < .001$) or Condition ($F(1, 29) = 3.75$, $p = .06$, $\eta^2G = .003$). The Condition × Target Type interaction was also non-significant ($F(1, 29) = 0.73$, $p = .40$, $\eta^2G < .001$).

Repeated-measures ANOVA on accuracy showed a significant main effect of Target Type ($F(1, 29) = 4.07$, $p = .05$, $\eta^2G = .008$), with higher accuracy for the related targets ($M = 0.94$) than for the unrelated targets ($M = 0.93$), but no significant main effect of Condition ($F(1, 29) = 0.03$, $p = .87$, $\eta^2G < .001$). The Condition × Target Type interaction was also non-significant ($F(1, 29) = 0.09$, $p = .76$, $\eta^2G < .001$).

N400

ERPs time-locked to the question prompt onset are shown in Figure 2A. Figure 2B (left) shows amplitude box plots for the extracted N400 amplitudes. Repeated-measures ANOVA on the N400 component (300–500 ms) showed a significant main effect of Target Type ($F(1, 29) = 17.11$, $p < .001$, $\eta^2_G = .02$), with unrelated targets eliciting more negative amplitudes (mean = -1.01 µV) than related targets (mean = -0.43 µV). A main effect of Condition reached significance ($F(1, 29) = 4.63$, $p = .04$, $\eta^2_G = .05$), with short condition showing more negative amplitudes (mean = -1.1 µV) than long (mean = -0.31 µV). Importantly, we observed a significant Condition × Target Type interaction ($F(1, 29) = 19.09$, $p < .001$, $\eta^2_G = .03$). Post hoc pairwise comparisons revealed that N400 amplitudes were significantly more negative for unrelated targets ($M = -0.93$ µV, $SD = 2.17$) than for related targets ($M = 0.22$ µV, $SD = 2.17$) in the long condition ($t(29) = 6.67$, $p < .001$, $p_{Bonf} < .001$), while in the short condition, no such difference was observed ($M_{related} = -1.18$ µV, $SD_{related} = 1.5$, $M_{unrelated} = 1.12$ µV, $SD_{unrelated} = 1.6$, $t(29) = -0.26$, $p = .8$, $p_{Bonf} = 1$).

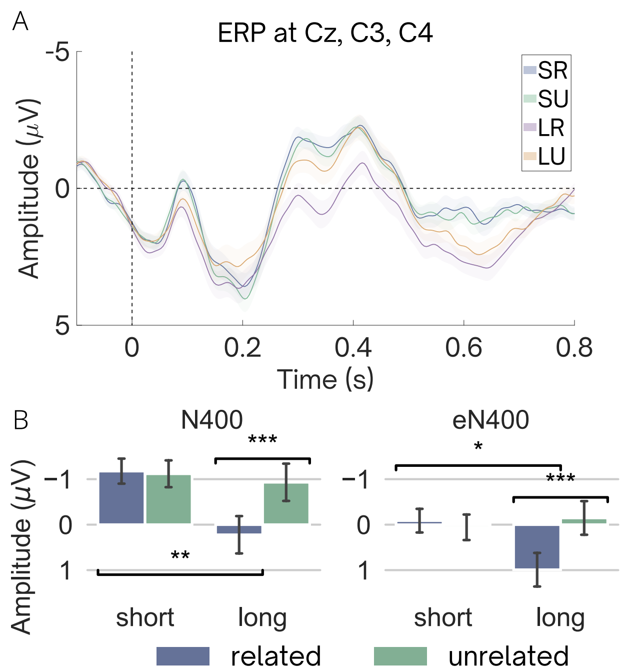

Figure 2: A. ERP results. ERPs time-locked to the onset of the question and baseline corrected at −200 to 0 ms for real words. Waveforms were averaged across central electrodes (C3, Cz, C4) for all conditions. SR: short condition, related target; SU: short condition, unrelated target; LR: long condition, related target; LU: long condition, unrelated target. B. N400 (left) and eN400 (right) amplitudes box plots. Asterisks indicate significant effects (*$p < .05$, **$p < .01$, ***$p < .001$, corrected for multiple comparisons) in a paired-samples t-test.

eN400

Amplitude box plots are presented in Figure 2B (right). Repeated-measures ANOVA on the eN400 amplitudes (100–300 ms) showed a significant main effect of Target Type ($F(1, 29) = 4.48$, $p = .04$, $\eta^2_G = .007$), with unrelated targets eliciting more negative amplitudes (mean = 1.39 µV) than related targets (mean = 1.64 µV). No significant main effect of Condition was observed ($F(1, 29) = 0.01$, $p = .92$, $\eta^2_G < .001$). The Condition × Target Type interaction was significant ($F(1, 29) = 13.5$, $p < .001$, $\eta^2_G = .02$). Pairwise comparisons showed that eN400 amplitudes were significantly more negative for unrelated targets ($M = -0.15$ µV, $SD = 1.9$) than for related targets ($M = 0.99$ µV, $SD = 1.9$) in the long condition ($t(29) = 4.52$, $p < .001$, $p_{Bonf} < .001$), while no such difference was observed in the short condition, ($M_{related} = -0.09$ µV, $SD_{related} = 1.37$, $M_{unrelated} = 0.06$ µV, $SD_{unrelated} = 1.5$, $t(29) = -1.2$, $p = .24$, $p_{Bonf} = .97$).

We conducted Pearson correlations between eN400 and N400 amplitudes for each experimental cell (2 Conditions × 2 Target Types), using Spearman correlation for the non-normal long-unrelated cell. All correlations were significant (Table 1), suggesting that for each individual participant, the amplitudes of the eN400 and N400 were highly correlated.

Table 1: Correlations between eN400 and N400 amplitudes across Conditions and Target Types.

Condition	Target Type	r	p
Short	Related	.41	.02
Short	Unrelated	.52	.003
Long	Related	.63	< .001
Long	Unrelated	.67	< .001

DDM

Focusing on the model that assumes both drift rate (v) and boundary separation (a) vary, for increasing N400 amplitude we observed significant positive drift rate (95% HDI [0.01, 0.03]; $P(v > 0) = 1$; Figure 3, top left). Boundary separation showed no significant effect (95% HDI [-0.003, 0.001], $P(a < 0) = .73$). For eN400, increasing amplitude led to negative boundary separation (95% HDI [-0.007, -0.002], $P(a < 0) = 1$; Figure 3, bottom right) and led to a non-significant effect for drift rate (95% HDI [-0.009, 0.009], $P(v > 0) = .52$).

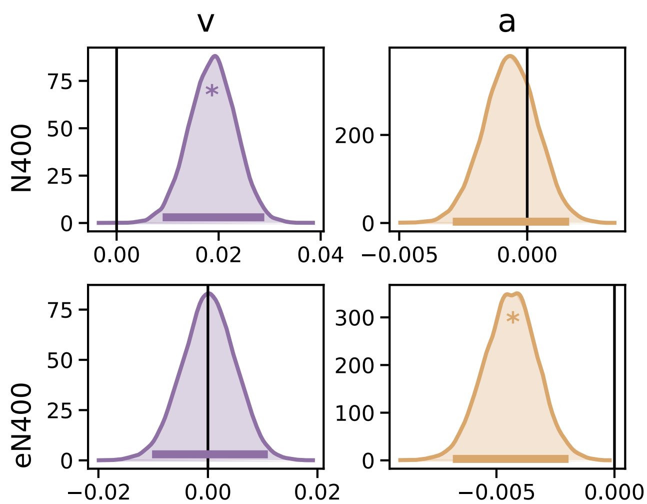

Figure 3: ERP-informed DDM results. Posterior density distributions of the drift rate (v) and boundary separation (a) for N400 (top) and eN400 (bottom). Horizontal lines below each distribution representing 95% HDIs.

Discussion

How does prediction manifest during semantic priming? This study addressed this question by examining the temporal dynamics of prediction-related neural activity, linking eN400 and N400 components to decision-making parameters via DDM.

First, consistent with Lau and colleagues (2013), only in the long prime condition where prediction is enhanced, we observed an early N400 effect for unrelated vs. related targets 100–300 ms after question onset. In the N400 time window, a similar pattern was identified: a significant priming-induced N400 effect was only found in the long prime condition. Here, importantly, these effects emerged in response to a minimal predictive context consisting of three semantically related primes, demonstrating that early prediction effects do not require sentence-level constraints (see Van Den Brink et al., 2001) and extending the findings to the semantic priming paradigm, as opposed to a global predictability manipulation in Lau et al. (2013).

Taken together, multiple lines of evidence suggest that eN400 effect could be an early manifestation of the N400, rather than a distinct component. First, we observed a strong correlation between eN400 and N400. Second, both eN400 and N400 effects were only found in the long condition, demonstrating that they may be modulated by the same contextual constraints in a similar way. Together, these findings support Lau et al.'s (2013) proposal that the eN400 could reflect early N400 activity, highlighting that predictive modulation can be elicited even by minimal statistical local buildup. Thus, in comparison with the traditional view of the N400 as a reflection of semantic retrieval (Kutas & Federmeier, 2011), our eN400 effect results indicate that the N400 component, together with its early instance, reflects rapidly unfolding predictive processes in language comprehension (Bornkessel-Schlesewsky & Schlesewsky, 2019).

Despite these similarities, our ERP-informed DDM implementation might indicate a functional dissociation of both components in their relevance to behavioral decision-making mechanisms. More positive classic N400 amplitudes were associated with higher drift rate, which indexes enhanced quality of semantic evidence that enters the decision processes. This does not invalidate the prediction-based interpretation of the N400; rather, it suggests that the classic N400 as a late, context-sensitive neural marker, relates most directly to evidence accumulation at least in the context of lexical decision. On the other hand, more positive eN400 amplitudes (prediction facilitation) correlated with smaller boundary separation, but not higher drift rate. Here, for trials with less negative eN400 amplitude, participants reverted to a more liberal decision-making strategy. This explanation aligns with predictive coding frameworks where prediction errors serve as control signals that modulate subsequent processing (Kuperberg & Jaeger, 2016). Boundary separation can be modulated by cognitive control mechanisms (Anders et al., 2017), which recent work has shown can be linked to prediction: control processes use predictions about upcoming demands to adjust behavior (Pan et al., 2024). Overall, this dissociation reveals temporally distinct influences of semantic processes on lexical decisions, demonstrating the multifaceted role of the N400 and its predictive negative component family (Bornkessel-Schlesewsky & Schlesewsky, 2019; Kuperberg & Jaeger, 2016; Ryskin & Nieuwland, 2023). It thus provides a mechanistic link between classic neural indices of linguistic prediction and latent decision computations.

Future studies using a task with more decision difficulty, such as a semantic categorization task or a task with degraded stimuli, could validate the DDM effects found in this study while producing stronger behavioral effects.

Together, our findings suggest that local predictive contextual buildup is sufficient to engage early context-sensitive neural activity and to modulate the classic N400 priming response. Furthermore, ERP-informed DDM provides initial evidence that neural signals tied to distinct processing phases may map onto different decision mechanisms: the eN400 component reflects strategic decision adjustment (boundary separation change), whereas the classic N400 most directly relates to evidence accumulation (drift rate change). This neurocomputational dissociation provides novel empirical evidence supporting the hierarchical predictive coding frameworks of language processing by specifying not only whether predictive context matters, but when it impacts semantic processing and which task-relevant decision mechanisms it changes.

Acknowledgments

AI-based language models (ChatGPT and Claude) were used solely for linguistic editing of the manuscript to improve clarity, conciseness and wording. AI models were not used for data analysis and interpretation.

References

Anders, R., Riès, S., Van Maanen, L., & Alario, F.-X. (2017). Lesions to the left lateral prefrontal cortex impair decision threshold adjustment for lexical selection. *Cognitive Neuropsychology*, *34*(1–2), 1–20. https://doi.org/10.1080/02643294.2017.1282447

Bornkessel-Schlesewsky, I., & Schlesewsky, M. (2019). Toward a Neurobiologically Plausible Model of Language-Related, Negative Event-Related Potentials. *Frontiers in Psychology*, *10*, 298. https://doi.org/10.3389/fpsyg.2019.00298

Brysbaert, M., Buchmeier, M., Conrad, M., Jacobs, A. M., Bölte, J., & Böhl, A. (2011). The Word Frequency Effect: A Review of Recent Developments and Implications for the Choice of Frequency Estimates in German. *Experimental Psychology*, *58*(5), 412–424. https://doi.org/10.1027/1618-3169/a000123

Delorme, A., & Makeig, S. (2004). EEGLAB: An open source toolbox for analysis of single-trial EEG dynamics including independent component analysis. *Journal of Neuroscience Methods*, *134*(1), 9–21. https://doi.org/10.1016/j.jneumeth.2003.10.009

Fengler, A., Xu, P., Bera, K., Omar, A., & Frank, M. J. (in prep.). *HSSM: A generalized toolbox for hierarchical bayesian estimation of computational models in cognitive neuroscience.*

Gomez, P., Perea, M., & Ratcliff, R. (2013). A diffusion model account of masked versus unmasked priming: Are they qualitatively different? *Journal of Experimental Psychology: Human Perception and Performance*, *39*(6), 1731–1740. https://doi.org/10.1037/a0032333

Grave, E., Bojanowski, P., Gupta, P., Joulin, A., & Mikolov, T. (2018). *Learning Word Vectors for 157 Languages* (arXiv:1802.06893). arXiv. https://doi.org/10.48550/arXiv.1802.06893

Kinoshita, S., De Wit, B., Aji, M., & Norris, D. (2017). Evidence accumulation in the integrated and primed Stroop tasks. *Memory & Cognition*, *45*(5), 824–836. https://doi.org/10.3758/s13421-017-0701-8

Klug, M., & Kloosterman, N. A. (2022). Zapline-plus: A Zapline extension for automatic and adaptive removal of frequency-specific noise artifacts in M/ EEG. *Human Brain Mapping*, *43*(9), 2743–2758. https://doi.org/10.1002/hbm.25832

Kuperberg, G. R., & Jaeger, T. F. (2016). What do we mean by prediction in language comprehension? *Language, Cognition and Neuroscience*, *31*(1), 32–59. https://doi.org/10.1080/23273798.2015.1102299

Kutas, M., & Federmeier, K. D. (2011). Thirty Years and Counting: Finding Meaning in the N400 Component of the Event-Related Brain Potential (ERP). *Annual Review of Psychology*, *62*(1), 621–647. https://doi.org/10.1146/annurev.psych.093008.131123

Lau, E. F., Holcomb, P. J., & Kuperberg, G. R. (2013). Dissociating N400 Effects of Prediction from Association in Single-word Contexts. *Journal of Cognitive Neuroscience*, *25*(3), 484–502. https://doi.org/10.1162/jocn_a_00328

Luka, B. J., & Van Petten, C. (2014). Prospective and retrospective semantic processing: Prediction, time, and relationship strength in event-related potentials. *Brain and Language*, *135*, 115–129. https://doi.org/10.1016/j.bandl.2014.06.001

Mueller, C. J., White, C. N., & Kuchinke, L. (2017). Electrophysiological correlates of the drift diffusion model in visual word recognition. *Human Brain Mapping*, *38*(11), 5616–5627. https://doi.org/10.1002/hbm.23753

Munding, M., Forgács, B., Lukics, K. S., & Lukács, Á. (2025). Individual Differences in Statistical Learning and Semantic Adaptation: An N400 Study. *Psychophysiology*, *62*(8), e70125. https://doi.org/10.1111/psyp.70125

Nieuwland, M. S., Barr, D. J., Bartolozzi, F., Busch-Moreno, S., Darley, E., Donaldson, D. I., Ferguson, H. J., Fu, X., Heyselaar, E., Huettig, F., Matthew Husband, E., Ito, A., Kazanina, N., Kogan, V., Kohút, Z., Kulakova, E., Mézière, D., Politzer-Ahles, S., Rousselet, G., … Von Grebmer Zu Wolfsthurn, S. (2020). Dissociable effects of prediction and integration during language comprehension: Evidence from a large-scale study using brain potentials. *Philosophical Transactions of the Royal Society B: Biological Sciences*, *375*(1791), 20180522. https://doi.org/10.1098/rstb.2018.0522

Nunez, M. D., Vandekerckhove, J., & Srinivasan, R. (2017). How attention influences perceptual decision making: Single-trial EEG correlates of drift-diffusion model parameters. *Journal of Mathematical Psychology*, *76*, 117–130. https://doi.org/10.1016/j.jmp.2016.03.003

Oostenveld, R., Fries, P., Maris, E., & Schoffelen, J.-M. (2011). FieldTrip: Open Source Software for Advanced Analysis of MEG, EEG, and Invasive Electrophysiological Data. *Computational Intelligence and Neuroscience*, *2011*, 1–9. https://doi.org/10.1155/2011/156869

Pan, Y., Guo, M., Jiang, Y., Liu, T., & Wu, X. (2024). The interplay of contextual and immediate uncertainty: Evidence for a common processing mechanism in prediction and cognitive control. *Current Psychology*, *43*(22), 19976–19984. https://doi.org/10.1007/s12144-024-05755-6

Peirce, J., Gray, J. R., Simpson, S., MacAskill, M., Höchenberger, R., Sogo, H., Kastman, E., & Lindeløv, J. K. (2019). PsychoPy2: Experiments in behavior made easy. *Behavior Research Methods*, *51*(1), 195–203. https://doi.org/10.3758/s13428-018-01193-y

Pion-Tonachini, L., Kreutz-Delgado, K., & Makeig, S. (2019). ICLabel: An automated electroencephalographic independent component classifier, dataset, and website. *NeuroImage*, *198*, 181–197. https://doi.org/10.1016/j.neuroimage.2019.05.026

Ratcliff, R., & Childers, R. (2015). Individual differences and fitting methods for the two-choice diffusion model of decision making. *Decision*, *2*(4), 237–279. https://doi.org/10.1037/dec0000030

Ratcliff, R., & McKoon, G. (2008). The Diffusion Decision Model: Theory and Data for Two-Choice Decision Tasks. *Neural Computation*, *20*(4), 873–922. https://doi.org/10.1162/neco.2008.12-06-420

Ryskin, R., & Nieuwland, M. S. (2023). Prediction during language comprehension: What is next? *Trends in Cognitive Sciences*, *27*(11), 1032–1052. https://doi.org/10.1016/j.tics.2023.08.003

Tumanyants, A., Straube, B., Mulert, C., & He, Y. (2025). *Local predictive context modulates evidence accumulation and boundary separation during semantic priming*. https://doi.org/10.31234/osf.io/n8egj_v4

Vallat, R. (2018). Pingouin: Statistics in Python. *Journal of Open Source Software*, *3*(31), 1026. https://doi.org/10.21105/joss.01026

Van Den Brink, D., Brown, C. M., & Hagoort, P. (2001). Electrophysiological Evidence for Early Contextual Influences during Spoken-Word Recognition: N200 Versus N400 Effects. *Journal of Cognitive Neuroscience*, *13*(7), 967–985. https://doi.org/10.1162/089892901753165872

Virtanen, P., Gommers, R., Oliphant, T. E., Haberland, M., Reddy, T., Cournapeau, D., Burovski, E., Peterson, P., Weckesser, W., Bright, J., Van Der Walt, S. J., Brett, M., Wilson, J., Millman, K. J., Mayorov, N., Nelson, A. R. J., Jones, E., Kern, R., Larson, E., … Vázquez-Baeza, Y. (2020). SciPy 1.0: Fundamental algorithms for scientific computing in Python. *Nature Methods*, *17*(3), 261–272. https://doi.org/10.1038/s41592-019-0686-2

Voss, A., Rothermund, K., Gast, A., & Wentura, D. (2013). Cognitive processes in associative and categorical priming: A diffusion model analysis. *Journal of Experimental Psychology: General*, *142*(2), 536–559. https://doi.org/10.1037/a0029459

Wiecki, T. V., Sofer, I., & Frank, M. J. (2013). HDDM: Hierarchical Bayesian estimation of the Drift-Diffusion Model in Python. *Frontiers in Neuroinformatics*, *7*. https://doi.org/10.3389/fninf.2013.00014